Graphene Oxide Synthesis and Characterization: Oxidation Effects on Structure and Stability

Yousra Ali Hussein[1], Jasim Mohammed Alzanganawee[1], Nabeel Ali Bakr[1] and Bassam M. Abood[2]
[1]*Department of Physics, University of Diyala, 32001 Baqubah, Iraq*
[2]*Chemical and Petrochemical Research Center, Corporation of Research and Industrial Development, 10070 Baghdad, Iraq*
{sciphyphd232410, Alzanganawee}@uodiyala.edu.iq, nabeelalibakr@yahoo.com
Bassam.abood1205@sc.uobaghdad.edu.iq

Keywords: Graphene Oxide (GO); Modified Hummers Oxidation Time; Structural Characterization.

Abstract: The aims of this study to produce graphene oxide (GO) with a modified Hummers' technique with oxidation durations of 8, 10, and 12 hur. XRD analyses revealed unique diffraction peaks consistent with the layered structure of GO. After 8 hur, two peaks appeared. One was at 2θ, corresponding to 11.1° and associated with the (001) plane. At 10 hur, peak were seen at 2θ = 10.3° (001), and after 12 hur, the peak shrank to 2θ = 8.1° (001) with d = 1.08 nm. Meanwhile, the peaks at 26.48° (002) and 31.05° (100) were relatively lower. FTIR studies revealed the presence of functional groups (O–H, C=O, C–O–C, and COOH). These groups became increasingly evident as the oxidation process proceeded for a prolonged period. The sheets were thin and distorted in FESEM/EDS images, and the amount of oxygen relative to carbon increased over time. TGA data show that sample B lost 84% of its weight at 500 °C, while sample A lost 83% of its weight at the same temperature. These samples were prepared in advance. Sample C, prepared over 12 hur, lost the least weight (47%), despite its prolonged oxidation. On the other hand, ZetaP experiments showed that the colloidal solutions of the prepared samples were stable (-35 to -52 mV). The sample prepared after 10 hours had an ideal balance between strength and oxidation.

1 INTRODUCTION

Nanoscience and nanotechnology concentrate on the production, characterization, and use of nanomaterials. Graphene has emerged as an extraordinary material owing to its unique characteristics. It is acknowledged as the thinnest, strongest, and most rigid material known, demonstrating exceptional thermal and electrical conductivity [1]. Graphene oxide (GO), a crucial derivative, has garnered considerable interest due to its economical manufacture, rapid synthesis, and scalability, rendering it exceptionally well-suited for practical applications [2] There are a few ways to make graphene oxide (GO), but the most common is to oxidize graphite using classic methods like the Brodie and Hummers methods. The oxidation processes add oxygen-containing functional groups to both sides of the graphite layers. This makes the space between the layers bigger and makes it easier for the graphite to spread out in polar solvents like water [2]. Graphene oxide's hydrophilic properties, which come from its surface functions, make it easier for it to interact with water, polar solvents, and hydrophilic polymers. This is different from pure graphene, which doesn't dissolve well in many solvents [3], [4]. Graphene exhibits remarkable theoretical features, such as a surface area of about 2600 m^2/g, charge mobility of around 200,000 $cm^2/V•s$, a Young's modulus close to 1.0 TPa, thermal conductivity of 5000 W/m•K, and optical transmittance near 97.7% [5]. Weak van der Waals forces, π–π stacking, and hydrogen bonding bind graphene oxide sheets to each other. This creates interlayer gaps (galleries) that are around 8 angstroms apart. These spaces could fit water molecules or other polar molecules [6]. The concentration of the oxidizing agent and the length of the oxidation process have a direct effect on how bad the structural defects in GO [7]. Conventional methods, like Brodie and Hummers, continue to be widely used for synthesizing graphene oxide [8]. The oxidation of graphite is influenced by several parameters, such as porosity, structural anisotropy, grain size,

crystallinity, radiation dosage, micropore dimensions, impurity presence, temperature, pressure, morphology, and the nature of the oxidizing gas [9]. Divergences in production techniques and raw materials result in notable discrepancies in oxidation behavior. The dimensions of the graphite particles significantly influence the extent of oxidation and the ultimate production of graphene oxide, with research demonstrating that smaller particles are more efficacious [1], [10]. The oxidation level of GO influences the residual functional groups and amplifies flaws on the substrate of the synthesized graphene [11]. This study utilized the modified Hummers method because of its precise control over oxidation levels and its ability to rectify structural issues. This will be achieved through a systematic analysis that correlates oxidation time with the structural and functional changes within the material [12]. This work aims to determine the effect of oxidation duration on the structural and thermal properties of graphene oxide produced by modified technique.

This objective is crucial because it aids in determining the ideal oxidation duration for achieving both moderate and complete oxidation levels. This directly affects the material's thermal, physical, and colloidal stability as well as its dispersion We employed several analytical techniques to assess the stability of the colloids. The techniques employed were X-ray diffraction (XRD), thermogravimetric analysis (TGA), Raman spectroscopy, Fourier transform infrared spectroscopy (FTIR), and zeta potential measurements.to assess colloidal stability. The results aim to provide a deeper understanding of the relationship between oxidation time and GO structure, and to identify the optimal conditions for preparing high-quality nanomaterials suitable for environmental, biomedical, and electronic applications .Although numerous studies have addressed the oxidation of graphite to produce graphene oxide (GO), most have focused on the effect of the oxidizing agent type or graphite size without providing a systematic analysis linking oxidation time to the structural and thermal transformations of the material. Shen et al. (2018) indicated that graphite size affects the degree of oxidation and reduction behavior, while Karins et al (2024). This study revealed that the oxidation duration and time spent on graphene are particularly important for modifying its chemical structure. There are not many studies directly linking the duration of oxidation to the properties of graphene, including its diffusion range, colloidal stability, and structure.

2 MATERIALS AND METHODS

2.1 Chemical and Reagents

All chemicals used are of high purity, including graphite flakes, potassium permanganate (99%RFCL), hydrogen peroxide (30% wt, Alpha Chemika (India), sulfuric acid (98%Loba chemie PVT.(India), hydrochloric acid (35%RANKEM), and phosphoric acid (99.9%Loba Chemie Pvt. (India), Ultrapure distilled water was used as a solvent in solution preparation, dilution, and washing to remove ionic impurities.

2.2 Experimental

Graphene oxide was prepared using a modified Hummers method. A 250 mL reaction vessel was first immersed in an ice bath. Concentrated sulfuric acid (molecular weight 98.08) was gradually added to 120 mL, stirring continuously at 500 rpm. Next, 14.5 mL of phosphoric acid (molecular weight 98.86) was gradually added to the mixture, stirring This improved the efficiency and stability of the oxidation process. Next, 1 gram of graphite powder was slowly added, making sure the temperature didn't go over 5 °C. This went on for 30 minutes to make sure the acid and graphite were completely mixed. The ratio of graphite to acid employed in this investigation was 1 g to 120 mL of H_2SO_4 and 14.5 mL of H_3PO_4 (1:120:14.5). This ratio was kept the same in all of the batches to make sure that the oxidation conditions stayed the same. The solution stayed dark gray, and the viscosity went up as the graphite particles settled out. 6 grams of potassium permanganate were then slowly added to the reaction mixture over the course of 10 minutes, with constant stirring and at a temperature below 20°C (with an ice bath present). After taking the ice bath away, the mixture was heated to 40°C on a hot plate while stirring it constantly at 500 rpm for 12 hours. To control oxidation, the ratio of graphite to $KMnO_4$ was fixed at 1:6 (g/g). The oxidation process was completed, and any excess chemicals that were oxidizing it were removed. After allowing the liquid to cool to room temperature 25°C, 100 ml of deionized water was gradually added to dilute it. Then, 10 ml of 30% hydrogen peroxide (H2O2) was slowly added. With the addition of the components, the color of the solution changed from dark brown to pale yellow within 15 minutes. Oxidation was stopped. To eliminate any remaining oxidants, a mixture of graphite and H_2O_2 at a ratio of 1:10 (g/ml) 30% was used. Adding 100 ml of deionized water further

diluted it. While continuously stirring the mixture, three 50-ml batches of hydrochloric acid (HCl, 35-38%, gable weight 36.46) were added. The solution was placed in tubes and swirled at 4000 rpm for 15 minutes. Simply put, the overlying liquid was repeatedly flushed with deionized water until its pH reached 7. Finally, the graphene oxide was left to dry for 1 day at 25°C. The ratio of the wash solution to graphene oxide was fixed at 1:250 (g/ml) until the pH of the filtrate approached 7.

2.3 Sedimentation Assessment

1 mg of graphene oxide was dissolved in 3 mL of deionized water, and the mixture was then exposed to bath sonication for 15 minutes in order to conduct visual sedimentation experiments.

2.4 Characterization

The graphene oxide (GO) sample's structure, shape, temperature, and particle characteristics were ascertained using a variety of techniques.

To examine the crystals, X-ray diffraction (XRD) was employed. A Shimadzu Lab-X XRD-6000 from Japan was equipped with a Cu K± radiation source (λ = 1.5405 Å), operating at 30 kV and 20 mA. The angular range (2θ) was designed to range from 20° to 80° at a speed of 2 cm/min. The graphene oxide grains were pressed together to form a flat surface before being measured Further Infrared Spectroscopy (FTIR).

FTIR spectra were recorded using two instruments: a Shimadzu IRAffinity-1 (Japan) and a PerkinElmer Frontier (USA).

GO samples were mixed with KBr at a spectral purity of 1 wt% GO to 99 wt% KBr and examined using ATR mode at room temperature. Raman Spectroscopy. Raman spectra were obtained using a Renishaw 2000 (UK) equipped with a 532 nm excitation laser. GO granules were placed on glass slides and scanned three times for 10 seconds each to minimize fluorescence interference. The spectral range covered 1000–5000 cm^{-1}.

Field Emission Scanning Electron Microscopy (FESEM) and Energy Dispersive X-ray Spectroscopy (EDXS): Surface morphology and elemental mapping were analyzed utilizing a FE-SEM (Mira3-XMU, TESCAN, Japan). EDXS analysis was performed at an accelerating voltage of 10.0 kV and a working distance of 15 mm. Samples were affixed to carbon tape and sputter-coated with a Pd/Au alloy utilizing a Polaron Instruments SEM Coating System (Model E5100) for 30 seconds.

Thermal stability was evaluated using a TGA Q-500 from TA Instruments. GO samples were placed in DSC-specific platinum vessels with perforated lids and heated in a nitrogen environment at 10°C/min to 1000°C.

Elements Analysis: used a German Elementar Vario Micro Cube analyzer to figure out the quantitative components composition. We used subtraction to find out how much oxygen was in the air.

Zeta Potential Assessment: A Zeta Plus from To ensure sure the graphene oxide samples stay stable in water, The United States-based business Brookhaven Instruments Corporation was utilized. A red diode laser with a power of 30 mW.

3 RESULTS AND DISCUSSION

3.1 XRD Analysis

Graphene oxide (GO) crystallizes, and the distance between its layers is affected by the time it takes to oxidize. We used X-ray diffraction (XRD) to investigate this. This method provides a clear picture of the structure's organization and the average spacing of the atoms, Figure 1.a shows the sample prepared after 8 hours. There is a clear peak at 2θ = 11.1°, the (001) plane, with a d-spacing of 0.79 nm. The addition of functional groups containing oxygen widens the gap between the layers. The broad, weak peak at 27.5°, corresponding to the (002) plane with a d-spacing of approximately 0.32 nm, indicates the presence of fewer layered graphene sheets with lower crystallinity than pure graphite [13] In Figure 1.b, the sample produced after 10 hours shows a shift in the (001) peak at 2θ = 10°, indicating a higher oxidation level. The (002) peak remains at 26.5°, indicating that the interlayer stacking is only partially preserved. However, its broadening and decreased intensity indicate significant structural disorder and the formation of partially crystalline graphene oxide (GO) domains [14]. Figure 1.c, the sample produced after 12 hours shows that the (001) reflection has disappeared and a new peak has appeared at 2θ = 8.1°. This indicates that the interlayer spacing has increased since the use of so much oxygen. The (002) peak at 26.48° remains unchanged, indicating that the graphite layers have begun to change and transform into reduced graphene oxide (rGO) [15], [16]. As shown in Table 1, the (002) reflection did not completely disappear in any of the samples; rather, its position, shape, and intensity varied with oxidation time. This variation reflects the gradual

transformation from graphite to GO, and then to a partially reduced structure with prolonged oxidation. Therefore, the weak and broad appearance of the (002) reflection does not contradict its absence in pure graphite, but rather indicates complex structural changes related to the degree of oxidation, the number of layers, and the crystallite size. These results demonstrate that oxidation time plays a crucial role in determining the layered structure of graphene oxide, and that the sample prepared for 10 hours represents an ideal intermediate state, combining interlayer expansion with partial retention of crystalline order, thus enhancing the properties of GO for applications requiring a balance between dispersibility and structural stability.

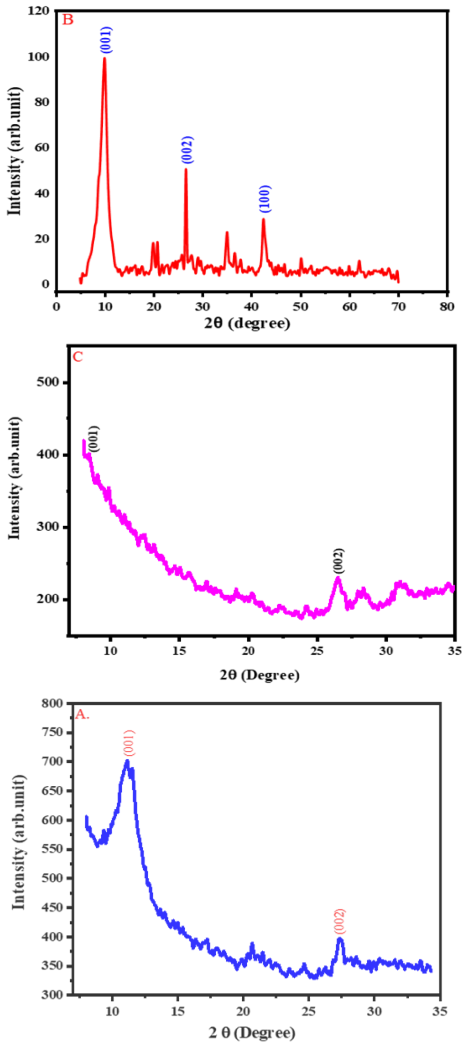

Figure 1: X-ray diffraction patterns of graphene oxide samples produced at different oxidation times: (a) 8 h, (b) 10 h, and (c) 12 h.

Table 1: X-ray diffraction results of (GO).

Sample	GO (8 h)	GO (10 h)	GO (12 h)
Peak position 2(θ)	11.16 27.54	10.3 26.5 42.2	8.1737 26.4868
FWHM β (°)	1.1509 1.564	1.594 1.812 0.084	0.9446 0.7557
d -Spacing nm	0.791 0.323	0.878 0.334 0.212	1.081 0.336
Crystallite Size (D) K λ/β cos θ (nm)	6.93 5.22	10.13 41.48 8.03	8.43 10.79
Average Crystallite Size D(nm)	5.65	23.21	9.61
hkl	(001) (002)	(001), (002) (100)	(001) (002)

3.2 Separate the FESEM Measurements from EDS

Figure 2. A. illustrates that the FESEM pictures indicate the generated graphene oxide after 8 hours of oxidation resulted in thin, wrinkled sheets. This exemplifies the properties the properties of graphene oxide and the attributes of its layered shape. The emergence of distortions and fissures is attributable to the incorporation of functional groups into the carbon lattice. The crumpled structure of graphene oxide signifies effective dispersion in water and polar liquids. This renders graphene oxide appropriate for biological purposes. Figure 2B The EDS analysis of GO after 8 hours the oxygen to carbon ratio is roughly 0.87, signifying a substantial level of oxidation. The existence of elements like silicon and sulfur signifies the presence of contaminants. The elevated oxygen content in the sample corroborates the FTIR findings, which indicated the existence of oxygen-rich functional groups [17]. The FESEM pictures in Figure 3 A demonstrate that the synthesized Go at 10 hours exhibit their typical thin, wrinkled, and layered sheet-like structures. These sheets frequently have a wrinkled or multilayered texture, which intrinsically enhances their extensive surface area. The photos further illustrate the capacity of these GO sheets to construct intricate, linked three-dimensional structures Figure 3 B. The EDS examination of GO corroborates the anticipated elemental composition, with carbon and oxygen as the predominant components, so proving the effective production of graphene oxide. The precise ratios of carbon to oxygen indicate the extent of oxidation and the

existence of diverse oxygen-containing functional groups on the surface Figure 4A. The SEM pictures in Figure 4A illustrate the production of graphene oxide conducted by the modified Hummers technique with an oxidation duration of 12 hours. The sheets have a wrinkled, lamellar structure due to oxygenated functional groups that deform the lattice and enhance interlayer space. These characteristics align with previous findings on oxidized graphene oxide and suggest that 12 hours of oxidation is adequate to produce multilayer graphene oxide with elevated surface area and reactive edges [18]. Figure 4B displays the EDS spectrum of GO synthesized with the modified Hummers technique (12 hours of oxidation), indicating that carbon and oxygen are the predominant constituents. The increased oxygen content verifies the inclusion of functional groups and signifies effective oxidation, but the diminished carbon portion implies π–π bond rupture and partial amorphization [19].

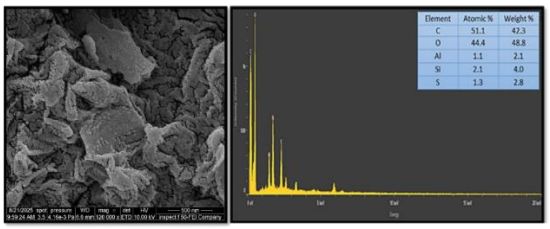

Figure 2: FESEM images and EDS. images of GO 8 hours.

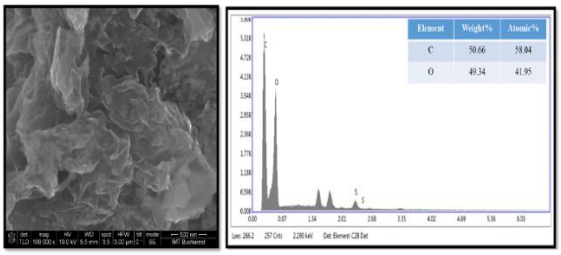

Figure 3: FESEM images and EDS of GO 10 hours.

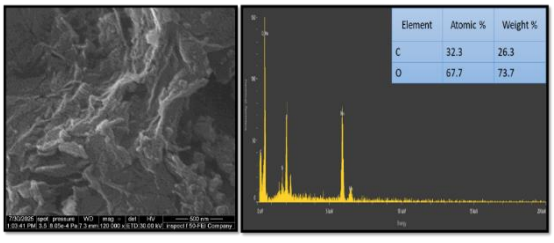

Figure 4: FESEM and Eds images of GO 12 hours.

3.3 Fourier Transform Infrared (FTIR) Spectroscopy

FT-IR spectra of graphene oxide GO samples, subjected to varying oxidation durations of 8, 10, and 12 hours, were obtained within the range of 4000–400 cm^{-1}, as seen in Figure 5. The spectra indicate the existence of distinctive vibrations of oxygen-containing functional groups, as seen in Table 2. A wide band at about 3434 cm^{-1} is ascribed to the vibrations of the hydroxyl group (O–H), which is also linked to the adsorbed water molecules interspersed between the layers. The two peaks at 2925 cm^{-1} and 2854 cm^{-1} correspond to the symmetric and asymmetric vibrations of aliphatic C–H bonds [20].

The peak at 1631 cm^{-1} corresponds to the vibration of the carbonyl group (C=O), whereas the peak at 1587 cm^{-1} is attributed to the C=C vibrations within the sp^2 bands of the graphene structure, aligning with the Raman spectrum, where the G-band peak signifies the carbon sp^2 vibrations [21].The peak at 1456 cm^{-1} also indicates the C–O vibrations, and the peak at 1269 cm^{-1} indicates the epoxide group (C–O–C), while the peak at 1113 cm^{-1} is due to the C–O–C vibrations of the alkoxy, and the peak at 877 cm^{-1} is associated with the out-of-plane aromatic (C–H) bends. It is worth noting that the intensity of peaks associated with oxygen groups, such as O–H, C=O, and C–O–C, increases with increasing oxidation time (10 and 12 hours), reflecting the increased incorporation of oxygen functional groups into the carbon network. In contrast, a relative decrease in the intensity of the C=C (sp^2) peak was observed with time, indicating increased disorder in the graphene structure. This is consistent with Raman results, where a high I_D/I_G ratio indicates an increased density of structural defects resulting from oxidation [Dreyer et al., 2010; Chen et al., 2013; Ferrari & Robertson, 2000 [22].

These results confirm that oxidation time plays a fundamental role in controlling the chemical and functional structure of graphene oxide, by balancing the incorporation of oxygen functional groups and the preservation of sp^2 domains. This directly affects the structural, optical, and chemical properties of the material.

The progressive increase in interlayer spacing (XRD) and the intensity of oxygen-containing groups (FTIR) are consistent with higher oxidation levels, as confirmed by the increased I_D/I_G ratio in Raman spectra.

3.4 Raman Spectrum of Go

Figure 6 shows the Raman spectra of graphene oxide samples produced at varying oxidation times, calibrated using a silicon reference peak at 520.7 cm^{-1}. The spectra were examined using a four-component model (D, D″, G, D′) in the range of 1200–1700 cm^{-1}, along with independent matching of the two-dimensional harmonic band between 2680–2730 cm^{-1}. The D band (approximately 1350 cm^{-1}) and the G band (1580–1600 cm^{-1}) were easily identified [23] The D″ band (approximately 1470 cm^{-1}) appeared after recalibration. The two-dimensional band at 2700 cm^{-1} is faint and cannot be measured, indicating that the graphite has very limited aggregation and poor crystallinity [20], [24]. Table 3 shows the Raman shifts of the main vibrational modes of samples A, B, and C. Sample A, prepared with 10 hours of oxidation, shows the most prominent defect-related features, with a D″ band at 1470 cm^{-1} and a G band at 1620 cm^{-1}. The intensity ratios (I_D/I_G), derived from the deviations of ±1.1, 2.3, and 1.5 for the samples, confirming their reproducibility. The sample deconvoluted conformations, showed standard subjected to 10 hours of preparation exhibited the most defect-induced disorder without significant band widening, aligning with the average time scale deduced from zeta potential, XRD, and FTIR analyses [25]. The increased defect density observed in Raman spectra corresponds to the variations in thermal stability detected by TGA, since higher oxidation and defect formation facilitate earlier weight loss during heating.

Table 2: Characteristics, vibrational modes and their energies prepared graphene oxides.

Wavenumber (cm^{-1})	Band Type	Ref
3431	O-H	[19]
2956-2854	CH2	[19]
1712	C=O	[20]
1631	C=O	[20]
1587	C=C	[20]
1465	C-O	[21]
1384	C-OH	[21]
1113	C-O-C	[21]
876-618	C-H	[21]
530-455	C-H	[21]

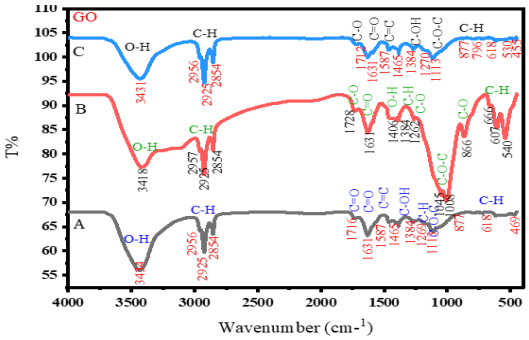

Figure 5: FTIR Spectroscopy of GO A (8hrs), B (10hrs), and C (12hrs).

Table 3: Raman shift are Simulated and match the Vibrational modes of D, G and 2D band.

Sample	Vibrational modes	Raman shift (cm^{-1})
A	D" band	1470 cm^{-1}
	G band	1620 cm^{-1}
	2D band	2680 cm^{-1}
B	D band	1344 cm^{-1}
	G band	1620cm^{-1}
	2D band	2720cm^{-1}
C	D band	1444cm^{-1}
	D" band	1670 cm^{-1}

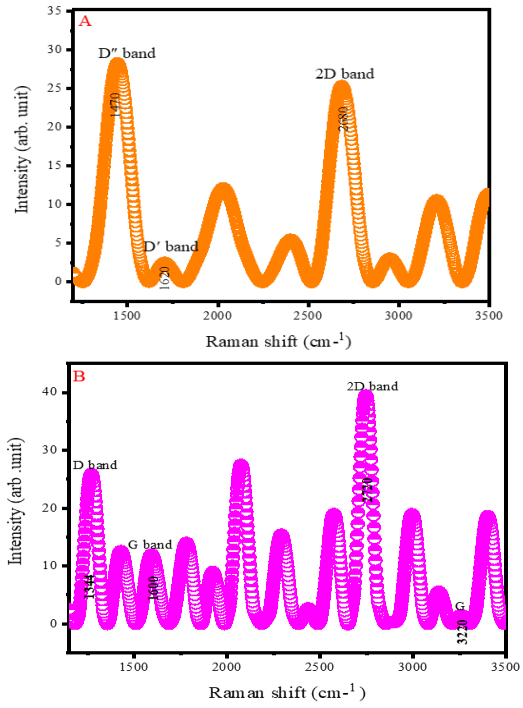

Figure 6: Raman spectra of graphene oxide (GO) samples produced at different oxidation times: (a) 8 h, (b) 10 h, and (c) 12 h.

3.5 Thermogravimetric Analyses (TGA)

The samples synthesized with the modified Hummer process for graphene oxide underwent thermal breakdown at temperatures reaching 1000°C in atmospheric air to examine their thermal characteristics. Figure 7, a, b and c illustrates graphs depicting molecular weight breakdown. The figures indicate that the synthesized graphene oxide combusted entirely before to attaining 1000°C. Sample B had a weight loss of 84%, surpassing Sample A loss of 83%, suggesting a more extensive disintegration of the graphene structure. Sample C exhibited the least mass loss, despite prolonged oxidation, suggesting surface saturation with functional groups without total structural failure. The principal mass loss of graphene oxide for Samples A and B is attributable to their decomposition temperatures ranging from 50-150°C, which accounts for a 53% loss of surface-adsorbed water, and from 150-300°C, which involves the decomposition of oxygen functional groups including hydroxyl, carboxyl, and epoxy, with the most significant loss occurring at 500°C. At 83% from Sample C at 100-250°C,[26] partial or total dissociation of the carbon lattice transpired to eliminate absorbed water and disintegrate the hydroxyl functional groups by 18% . The temperature range of 250-500°C resulted from the disintegration of oxygen groups, namely carboxyl-epoxy, connected to the carbon structure at a rate of 28%. At 500°C, the functional groupings disintegrated without total collapse at 47%. Graphene oxide, because to its elevated concentration of oxygen functional groups, necessitates a low energy threshold for breakdown. [27].

3.6 Zeta Potential Measurement

Figure 8 (a, b, and c) and Table 4 display zeta potential measurements of graphene oxide synthesized by the modified Hummers technique at varying oxidation durations 8, 10, and 12 hours. Zeta potential is a vital metric for analyzing the aggregation and dispersion behavior of particles in solution, as it indicates the degree of electrostatic repulsion among similarly charged particles, thereby serving to evaluate the stability of colloidal dispersions [28]. The samples had negative zeta potential values of −35.71 mV at 8 hours, −52.87 mV at 10 hours, and −21.23 mV at 12 hours. The negative values indicate that the particles possess a negative charge and lie within the moderate to high stability range, which inhibits fast sedimentation and facilitates the suspension of particles in the medium. The zeta potential measurements were conducted at pH levels between 2 and 12, the instrument's operational limits, with a 30-mW laser. The actual pH and ionic strength of the solution significantly impact the results, as pH affects the ionization of functional groups on the GO surface, while ionic strength influences the thickness of the electrical double layer, thereby altering the zeta potential and affecting dispersion behavior. The sample prepared after 10 hours was deemed ideal according to many metrics. It had the most significant negative zeta potential value (−52.87 mV), signifying robust electrostatic repulsion among particles, enhanced colloidal stability, and a more homogeneous particle dispersion.

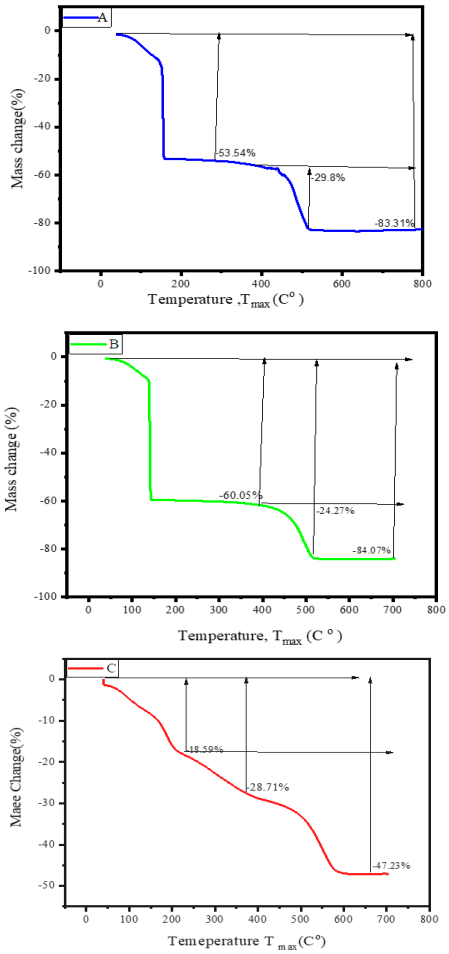

Figure 7: Thermogravimetric analysis (TGA) curves of graphene oxide (GO) samples synthesized at different oxidation durations: (A) 8 h, (B) 10 h, and (C) 12 h. The curves illustrate the thermal stability and decomposition behavior of GO.

Table 4: Zeta Potential results of GO.

Sample code	Zeta potential
A	-35.71
B	-52.87
C	-21.23

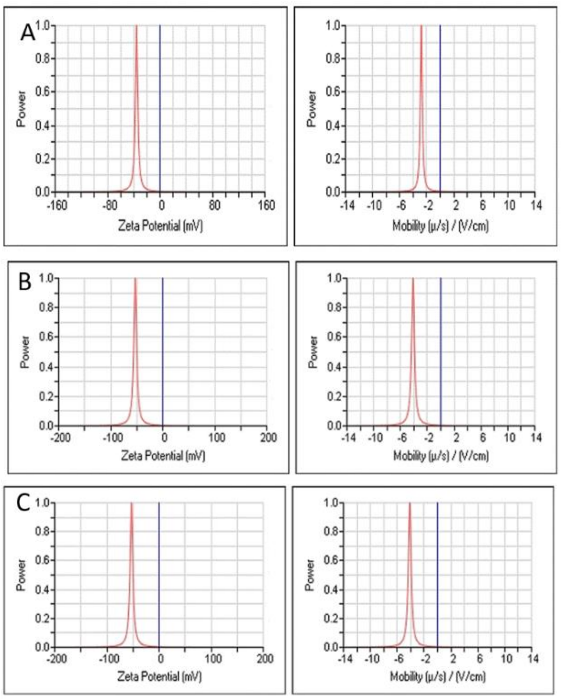

Figure 8: Zeta potential of graphene oxide (GO) samples produced at different oxidation times: (A) 8 h, (B) 10 h, and (C) 12 h.

4 CONCLUSIONS

Graphene oxide (GO) was effectively prepared with the modified Hummers technique with oxidation durations of 8, 10, and 12 hours. The oxidation duration was identified as a pivotal element affecting the structural, surface, and chemical properties of the resultant (GO) samples. XRD examination indicated that the sample processed for 8 hours exhibited partial oxidation while maintaining aspects of the original graphene structure. For 12 hours, had a higher incidence of structural flaws and diminished uniformity, whereas at 10 hours revealed an ideal equilibrium between oxidation level and structural integrity. This was corroborated by the beneficial interlayer expansion (d-spacing) evident in XRD patterns. The existence of several oxygen-containing functional groups was validated by FTIR spectra. Raman examination indicated a moderate structural defect ratio (I_D/I_G), corroborating the intermediate oxidation level at 10 hours. Zeta potential tests showed satisfactory colloidal stability for the fabricated samples. The samples registered negative zeta potential values of -35.71 mV at 8 hours, -52.87 mV at 10 hours, and -21.23 mV at 12 hours. These negative values indicate that the particles carry a negative charge and fall within a moderate to high stability range. Thermogravimetric analysis (TGA) revealed a notable disparity in thermal stability across the samples. Sample B had the greatest weight loss 84% after 10 hours at about 500 °C, followed by sample A with an 83% loss after 8 hours, whilst sample C demonstrated the least weight loss at 47% after 12 hours. These findings underscore the impact of oxidation duration on thermal behavior, with the 10-hour sample exhibiting better regulated breakdown. FESEM and EDS studies verified that the samples include thin, well-exfoliated sheets with a homogeneous oxygen distribution throughout the layers. The morphological and compositional findings further substantiate that the 10-hour oxidation procedure produces GO with advantageous physical and chemical characteristics. The findings indicate that oxidation duration significantly influences the physicochemical characteristics of graphene oxide produced by the modified Hummers technique. The oxidation for 10 h yields an excellent equilibrium among oxidation extent, defect density, and structural integrity in the examined samples. This setting yields well-exfoliated GO sheets characterized by plentiful oxygen functionalities, moderate defect density, excellent colloidal stability, and advantageous thermal properties. Consequently, GO produced during a 10-hour oxidation duration is the most appropriate for practical applications in industrial, environmental, and biological domains. These data will provide a reference to further study the nature of graphene oxide.

ACKNOWLEDGMENTS

The authors would like to express their sincere gratitude to the Department of Physics, College of Science, University of Diyala, for their continuous support and provision of the necessary facilities to conduct this research.

REFERENCES

[1] S. M. Hussein, T. Mubarak, S. A. Ridha, and J. Al-Zanganawee, "Synthesis and studying induction heating of Mn1-xZnxFe2O4 (x = 0-0.5) magnetic nanoparticles for hyperthermia treatments," Key Eng. Mater., vol. 882, pp. 200-2021, 2021, [Online]. Available: https://doi.org/10.4028/www.scientific.net/KEM.882.200.

[2] B. Ankamwar and F. Surti, "Water soluble graphene synthesis," Chem. Sci. Trans., vol. 1, no. 3, pp. 500-507, 2012, [Online]. Available: https://doi.org/10.7598/cst2012.155.

[3] S. KJ, "Studies on structural, linear and non-linear optical properties of graphene oxide and reduced graphene oxide," St. Teresa's Autonomous College, Ernakulam, 2023.

[4] R. R. Nair et al., "Fine structure constant defines visual transparency of graphene," Science, vol. 320, no. 5881, pp. 1308-1308, 2008, [Online]. Available: https://doi.org/10.1126/science.1156965.R.

[5] H. Li and K. Leifer, "Determining the elasticity of graphene," Image Microsc., vol. 21, pp. 32-34, 2019.

[6] W. Chen et al., "The preparation and application of polymer/graphene nanocomposites," Emerg. Mater. Res., vol. 9, no. 3, pp. 943-959, 2020, [Online]. Available: https://doi.org/10.1680/jemmr.17.00031.

[7] M. Ayán-Varela et al., "A quantitative analysis of the dispersion behavior of reduced graphene oxide in solvents," Carbon, vol. 75, pp. 390-400, 2014, [Online]. Available: https://doi.org/10.1016/j.carbon.2014.04.031.

[8] J. Al-Zanganawee et al., "On the physical properties of inverted photovoltaic structures based on P3OT:F-SWCNTs active layer," J. Ovonic Res., vol. 14, pp. 287-292, 2018.

[9] K. Anagnostou et al., "An extensive case study on the dispersion parameters of HI-assisted reduced graphene oxide and its graphene oxide precursor," J. Colloid Interface Sci., vol. 580, pp. 332-344, 2020, [Online]. Available: https://doi.org/10.1016/j.jcis.2020.07.017.

[10] D. R. Dreyer, S. Park, C. W. Bielawski, and R. S. Ruoff, "The chemistry of graphene oxide," Chem. Soc. Rev., vol. 39, no. 1, pp. 228-240, 2010, [Online]. Available: https://doi.org/10.1039/B917103G.

[11] I. Karnis et al., "Varying the degree of oxidation of graphite: effect of oxidation time and oxidant mass," Phys. Chem. Chem. Phys., vol. 26, no. 13, pp. 10054-10068, 2024, [Online]. Available: https://doi.org/10.1039/d3cp05268k.

[12] L. Shen et al., "Analysis of oxidation degree of graphite oxide and chemical structure of corresponding reduced graphite oxide by selecting different-sized original graphite," RSC Adv., vol. 8, no. 31, pp. 17209-17217, 2018, [Online]. Available: https://doi.org/10.1039/C8RA01486H.

[13] S. Rao et al., "Reduced graphene oxide: Effect of reduction on electrical conductivity," J. Compos. Sci., vol. 2, no. 2, p. 25, 2018, [Online]. Available: https://doi.org/10.3390/jcs2020025.

[14] H. Meng et al., "Cu2O nanorods modified by reduced graphene oxide for NH3 sensing at room temperature," J. Mater. Chem. A, vol. 3, no. 3, pp. 1174-1181, 2015, [Online]. Available: https://doi.org/10.1039/C4TA06024H.

[15] A. K. Swain and D. Bahadur, "Enhanced stability of reduced graphene oxide colloid using cross-linking polymers," J. Phys. Chem. C, vol. 118, no. 18, pp. 9450-9457, 2014.

[16] W. Liu and G. Speranza, "Tuning the oxygen content of reduced graphene oxide and effects on its properties," ACS Omega, vol. 6, no. 9, pp. 6195-6205, 2021, [Online]. Available: https://doi.org/10.1021/acsomega.0c05578.

[17] P. Mrkwitschka et al., "Standardized chemical composition analysis of graphene oxide flakes with SEM/EDS and XPS works reliably," Microsc. Microanal., vol. 31, no. Suppl. 1, p. ozaf048.267, 2025, [Online]. Available: https://doi.org/10.1093/mam/ozaf048.267.

[18] S. Pei and H.-M. Cheng, "The reduction of graphene oxide," Carbon, vol. 50, no. 9, pp. 3210-3228, 2012, [Online]. Available: https://doi.org/10.1016/j.carbon.2011.11.010.

[19] D. C. Marcano et al., "Improved synthesis of graphene oxide," ACS Nano, vol. 4, no. 8, pp. 4806-4814, 2010, [Online]. Available: https://doi.org/10.1021/nn1006368.

[20] G. Surekha et al., "FTIR, Raman and XRD analysis of graphene oxide films prepared by modified Hummers method," J. Phys.: Conf. Ser., vol. 1495, no. 1, p. 012012, 2020, [Online]. Available: https://doi.org/10.1088/1742-6596/1495/1/012012.

[21] D. He et al., "Mechanism of a green graphene oxide reduction with reusable potassium carbonate," RSC Adv., vol. 5, no. 16, pp. 11966-11972, 2015, [Online]. Available: https://doi.org/10.1039/C4RA16794A.

[22] A. Ramya, B. Manoj, and A. N. Mohan, "Extraction and characterization of wrinkled graphene nanolayers from commercial graphite," Asian J. Chem., vol. 28, no. 5, pp. 1031-1036, 2016.

[23] G. G. Politano and C. Versace, "Recent advances in the Raman investigation of structural and optical properties of graphene and other two-dimensional materials," Crystals, vol. 13, no. 9, p. 1357, 2023, [Online]. Available: https://doi.org/10.3390/cryst13091357.

[24] T. Alves et al., "Review of scientific literature and standard guidelines for the characterization of graphene-based materials," J. Mater. Sci., vol. 59, no. 32, pp. 14948-14980, 2024, [Online]. Available: https://doi.org/10.1007/s10853-024-09158-3.

[25] T. Parker et al., "In situ Raman and Fourier transform infrared spectroscopy studies of MXene−electrolyte interfaces," ACS Nano, 2025, [Online]. Available: https://doi.org/10.1021/acsnano.4c11652.

[26] F. Farivar et al., "Unlocking thermogravimetric analysis (TGA) in the fight against fake graphene materials," Carbon, vol. 179, pp. 505-513, 2021, [Online]. Available: https://doi.org/10.1016/j.carbon.2021.04.059.

[27] S. Gadipelli and Z. X. Guo, “Graphene-based materials: Synthesis and gas sorption, storage and separation,” Prog. Mater. Sci., vol. 69, pp. 1-60, 2015, [Online]. Available: https://doi.org/10.1016/j.pmatsci.2014.10.004.

[28] S. Mourdikoudis, R. M. Pallares, and N. T. Thanh, “Characterization techniques for nanoparticles: Comparison and complementarity upon studying nanoparticle properties,” Nanoscale, vol. 10, no. 27, pp. 12871-12934, 2018, [Online]. Available: https://doi.org/10.1039/C8NR02278J.